Tellus (1980), *32*, 500–510

Atmospheric energy fluxes over Europe

By M. ALESTALO and E. HOLOPAINEN, *Department of Meteorology, University of Helsinki, Hallituskatu 11-13, 00100 Helsinki 10, Finland*

(Manuscript received February 1; in final form April 14, 1980)

ABSTRACT

Horizontal fluxes of atmospheric energy (sensible and latent heat, potential and kinetic energy) are computed at European aerological stations between the surface and the 150 mb level for the period 1974–1976. The fluxes are divided into their mean flow and transient eddy contributions. The main emphasis is given to the computed transient eddy fluxes and their physical and synoptic interpretation.

The vertically integrated transient eddy fluxes of sensible heat and latent heat are essentially down-gradient and reflect the "mixing" caused by the large-scale atmospheric turbulence.

The transient eddy flux of sensible heat in the upper troposphere over western Europe in winter is found to be southward and up-gradient. By using a simple averaging technique it is shown that this up-gradient flux is due mainly to fluctuations with a period of less than 1 month. A synoptic example is presented showing a large-amplitude wave, typical in situations when formation of cut-off lows and shearlines takes place in the upper troposphere. In this case there is a negative spatial correlation between temperature and the meridional wind component. This kind of phenomenon, which is common over western Europe, is at least partially responsible for the observed up-gradient component of the sensible heat flux by transient eddies.

1. Introduction

Much attention has been paid to the evaluation of atmospheric fluxes of energy, momentum, and moisture in the zonally averaged scheme during the past decades. The most comprehensive documentations of these statistics are those of Oort and Rasmusson (1971) and Newell et al. (1972, 1974).

Recently, however, effort has been put into the evaluation of atmospheric statistics for smaller scales. The spectral dependence of these statistics on different space and time scales has also become an object of study. The works of Blackmon (1976) and Lau (1978) are examples in this direction. This new approach is essential because local atmospheric conditions may differ considerably from the zonal average.

Following the latter approach, some characteristic features of the atmospheric energy fluxes over Europe are presented in this study. They are based on twice daily radiosonde data for 3 years (1974–1976) between the surface and the 150 mb levels. The main emphasis is placed on transient eddy fluxes. The fluxes are presented in vector format and their relations with the horizontal distribution of some relevant quantities are discussed.

An interesting phenomenon that has recently received attention is the observed southward transient eddy flux of sensible heat in the upper troposphere over western Europe (and western North America). Its existence was shown originally by Priestley (1949) and has later been discussed by Speth (1978), Lau (1978) and Opsteegh and van den Dool (1979). A rough time-spectrum of this flux in the vicinity of the tropopause is studied in this paper by dividing the total flux into components arising from the fluctuations, the period of which is shorter/longer than a month. At the end of the article a synoptic interpretation of the southward flux is suggested with reference to atmospheric phenomena as found on synoptic charts.

Choosing Europe as the computational area allows the use of one of the densest parts of the global aerological observation network. The fact that many types of radiosondes are used in this area, leads to spurious systematic temperature and height differences in the upper levels between stations (Spackmann, 1978). However, these differences have hardly any effect on the transient eddy statistics discussed here.

2. Method

The time–mean total flux of a quantity, s, may be divided into a component associated with the mean motion and a component associated with transient motions:

$$\overline{s\mathbb{v}} = \bar{s}\,\bar{\mathbb{v}} + \overline{s'\mathbb{v}'}, \tag{1}$$

where the bar denotes time–mean value and the prime a deviation from this ($\mathbb{v}$ denotes the horizontal velocity). The transient eddy flux, evaluated at a certain station and at a certain pressure level, roughly includes the effect of all fluctuations longer than the period between successive observations and shorter than the averaging period.

In order to make an approximate study of the spectrum of the transient eddy fluxes, the total covariance is divided into two parts

$$\overline{s'\mathbb{v}'} = \overline{\tilde{s}'\,\tilde{\mathbb{v}}'} + \overline{\widetilde{s''\mathbb{v}''}}, \tag{2}$$

where the wavy bar denotes a monthly mean value and the double prime a deviation from this. The first right-hand side term (i.e. the covariance of the monthly mean values) roughly includes the contribution of fluctuations with periods longer than a month, and the second right-hand side term the contribution of fluctuations shorter than a month.

For the sake of brevity, the following symbols are used hereafter

$$\mathbb{F}_S = \int_{150}^{p_s} c_p T \mathbb{v} \frac{dp}{g} \quad \text{(flux of sensible heat)}$$

$$\mathbb{F}_P = \int_{150}^{p_s} \Phi \mathbb{v} \frac{dp}{g} \quad \text{(flux of potential energy)}$$

$$\mathbb{F}_L = \int_{150}^{p_s} Lq \mathbb{v} \frac{dp}{g} \quad \text{(flux of latent heat)}$$

$$\mathbb{F}_K = \int_{150}^{p_s} k \mathbb{v} \frac{dp}{g} \quad \text{(flux of kinetic energy)}$$

(The notation is conventional.) We can thus write the vertically integrated horizontal atmospheric energy flux $\mathbb{F}_A$ at any moment as

$$\mathbb{F}_A = \mathbb{F}_S + \mathbb{F}_L + \mathbb{F}_P + \mathbb{F}_K. \tag{3}$$

We further denote

$$\bar{\mathbb{F}} = \bar{\mathbb{F}}^M + \bar{\mathbb{F}}^T, \tag{4}$$

where $\bar{\mathbb{F}}$ refers to the time–mean flux, $\bar{\mathbb{F}}^M$ to the flux due to the mean flow and $\bar{\mathbb{F}}^T$ that due to the transient eddies.

3. Preparation of data

The basic material for this study was received from the Swedish Meteorological and Hydrological Institute, where original temperature, humidity, geopotential and wind data from the Northern Hemisphere were collected and stored on magnetic tapes. The aerological stations, for which energy fluxes were computed, are seen in Fig. 1, which actually shows the availability of wind observations at 300 mb for the whole 3-year period; the numbers slightly exceed the corresponding numbers reported by Kung (1966) in his investigation of the kinetic energy balance for North America.

The data were available for geopotential, temperature. dew point deficit, wind direction and speed at standard and significant levels between 1000 and 150 mb. From the original files new ones were generated consisting of geopotential, temperature, specific humidity and zonal and meridional wind components at the following levels: the surface, 1000, 950, 900, 850, 800, 700, 600, 500, 400, 300, 200, and 150 mb. The values at levels 950, 900, 800 and 600 mb were interpolated. A detailed description of the interpolation technique is given in Alestalo (1979).

In the next stage of data preparation the obvious errors due to coding, telecommunication and other causes were manually eliminated by inspecting monthly values of the standard deviation of geopotential, temperature, specific humidity and wind components and listing values departing more than three standard deviations from the corresponding mean value. Finally, the wind observations were checked in order to eliminate unrealistic wind shears by defining upper limits for the shear in every layer.

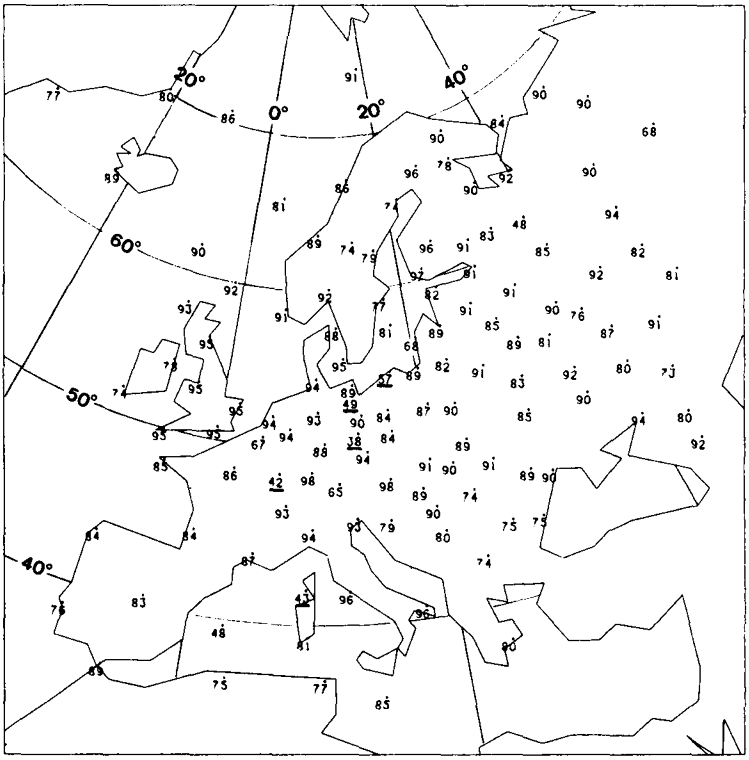

Fig. 1. The percentage of available wind observations at 300 mb for the period 1974–1976. The underlined numbers refer to stations with only one observation a day.

The calculations made with the basic data consisted of computations of monthly, seasonal, and annual statistics for aerological stations in Fig. 1. At each level the following quantities were determined:

Number of observations	Time mean and standard deviation	Fluxes
$N(z)$	$\bar{z}$, $\sigma(z)$	
$N(T)$	$\bar{T}$, $\sigma(T)$	
$N(q)$	$\bar{q}$, $\sigma(q)$	
$N(z,\mathbb{V})$	$\bar{z}^v$, $\sigma^v(z)$	$\overline{z\mathbb{V}}$, $\bar{z}^v\bar{\mathbb{V}}$, $\overline{z'\mathbb{V}'}$
$N(T,\mathbb{V})$	$\bar{T}^v$, $\sigma^v(T)$	$\overline{T\mathbb{V}}$, $\bar{T}^v\bar{\mathbb{V}}$, $\overline{T'\mathbb{V}'}$
$N(q,\mathbb{V})$	$\bar{q}^v$, $\sigma^v(q)$	$\overline{q\mathbb{V}}$, $\bar{q}^v\bar{\mathbb{V}}$, $\overline{q'\mathbb{V}'}$
$N(\mathbb{V})$	$\bar{u}$, $\sigma(u)$	$\overline{u^2}$, $\bar{u}^2$, $\overline{u'^2}$
	$\bar{v}$, $\sigma(v)$	$\overline{v^2}$, $\bar{v}^2$, $\overline{v'^2}$
	$\bar{k}$, $\sigma(k)$	$\overline{k\mathbb{V}}$, $\bar{k}\bar{\mathbb{V}}$, $\overline{k'\mathbb{V}'}$

Here the upper index "v" for a quantity refers to simultaneous observations of that quantity and wind. At the European radiosonde stations, wind observations in the upper layers are absent more often than those for temperature and height. Therefore, for example, $N(T,\mathbb{V})$ is typically smaller than $N(T)$ and $\bar{T}^v$ is not exactly the same as $\bar{T}$, although the differences are not very large. For the partitioning of the flux according to eq. (1) the difference can be significant, however.

4. Vertically-integrated energy fluxes

4.1. *Annual-mean conditions*

The areal distribution of the vertically integrated annual-mean total flux of energy $\bar{\mathbb{F}}_A$ (Fig. 2a) strongly reflects the pattern of mean horizontal wind vectors $\bar{\mathbb{V}}$. Thus, the pattern of $\bar{\mathbb{F}}_A$ is characterized by a zonality and a small trough over central Europe. For the mean fluxes of the different energy components ($\bar{\mathbb{F}}_S$, $\bar{\mathbb{F}}_L$, $\bar{\mathbb{F}}_P$, $\bar{\mathbb{F}}_K$, not shown) the general features are very similar. Differences only arise due to the vertical distribution of each energy component depending on whether the lower troposphere (as in the case of $\bar{\mathbb{F}}_L$) or upper troposphere

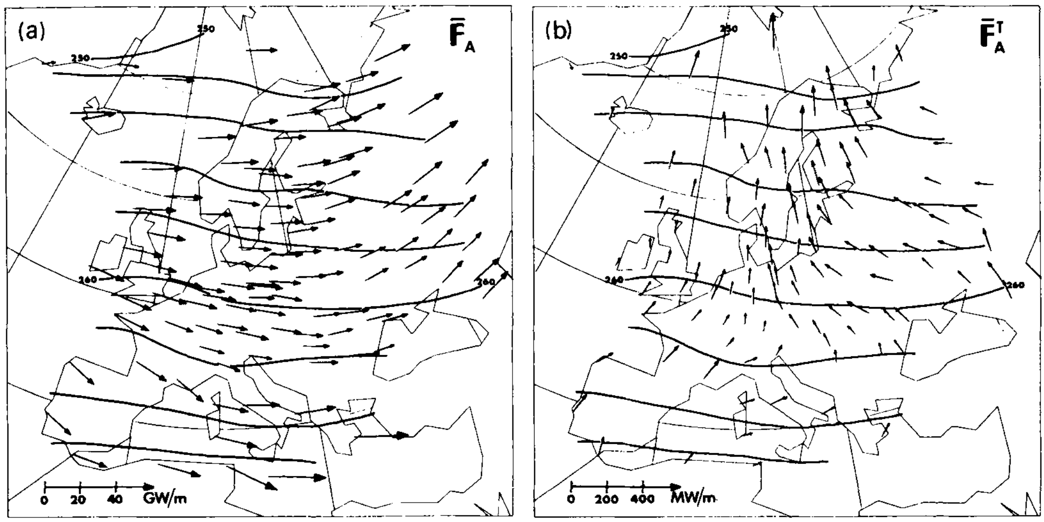

Fig. 2. Mean annual flux of total energy. (a) the vertically integrated annual–mean total flux of total energy ($\mathbb{F}_A$, eq. (3)). The analysis of the vertically averaged total energy, $c_pT + Lq + k$, between the surface and 150 mb for the period 1974–1976 is also shown. Unit of energy: 10^3 J kg^{-1}. (b) As in (a) but for the transient eddy flux of total energy.

(as in the case of $\bar{\mathbb{F}}_P$) is dominating. Basically, the similarity between the mean energy flux and mean velocity reflects the fact that $\bar{\mathbb{F}}_A$ is mainly determined by $\bar{\mathbb{F}}_A^M$.

The field of the vertically integrated transient eddy flux of total energy $\bar{\mathbb{F}}_A^T$ (Fig. 2b) differs both qualitatively and quantitatively from that of $\bar{\mathbb{F}}_A^M$. The flux vectors are generally directed to the north and are two orders of magnitude smaller than $\bar{\mathbb{F}}_A^M$ vectors. The northward transient eddy flux of the total energy may be understood as being due to the characteristic effect of baroclinic waves in mixing subtropical and polar air. The former is generally associated in these waves with larger total energies and northward motion while the latter is characterized by a negative energy anomaly and southward flow. Statistically this leads to northward eddy flux of total energy.

A comparison of the computed fluxes over Europe with zonally averaged conditions for respective latitudes (e.g. Oort and Rasmusson, 1971) shows striking differences. The meridional flux associated with the time–mean motion, quite important on a local scale, makes only a very small contribution in the zonally averaged case. This means that the zonal average of the meridional component of $\bar{\mathbb{F}}_A^M$ at a particular latitude represents only a small net effect of the conditions which vary in a wave-like fashion with longitude. Therefore, in the zonally averaged conditions the transient eddy fluxes dominate in the middle and high latitudes, particularly in the annual–mean picture.

If the budgets of atmospheric energy are considered, the energy fluxes themselves are not as important as the divergences associated with them. It appears, as will be shown in a later paper, that the divergence of energy flux by mean motion is generally not much larger than that of the transient eddy flux (see also Behr and Speth, 1977). Thus the mean-flow fluxes are mainly non-divergent and typically contain a large eastward flux component practically everywhere in the midlatitude westerlies. The splitting of flux vectors into non-divergent and irrotational parts was not done here because of the difficulty of specifying suitable boundary conditions (for hemispheric scale this has been done by Lau and Wallace, 1979). It must also be pointed out that the non-divergent flux components are not unimportant: when studying regional budgets of second-order quantities, such as temperature variance $\overline{T'^2}$, total fluxes (and not only irrotational flux components) are needed.

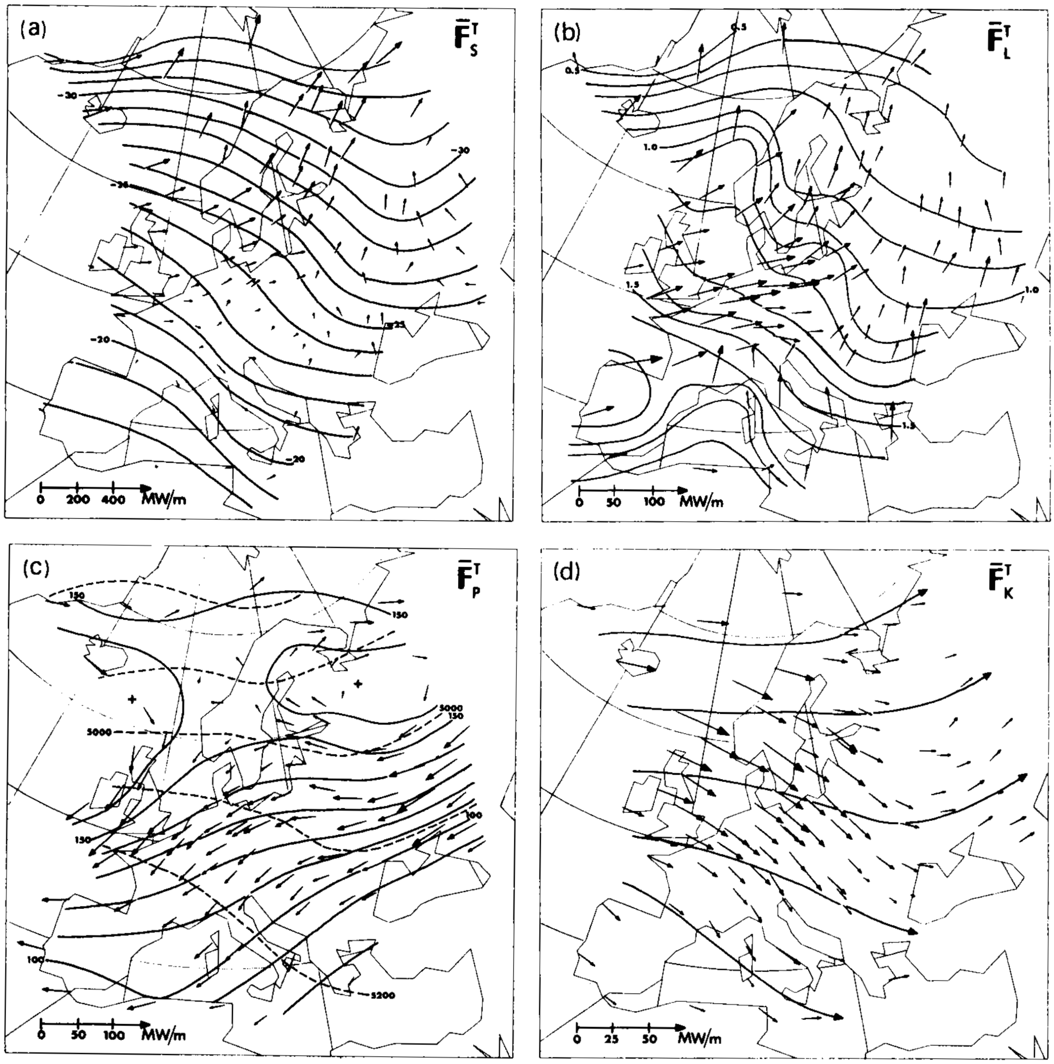

Fig. 3. Transient eddy energy fluxes in winter. (a) The vertically integrated transient eddy flux of sensible heat in winter and the analysis of vertically averaged temperature between the surface and 150 mb for the period 1974–1976. Contour interval is 1 °C. (b) As in (a) but for the latent heat flux and specific humidity. Contour interval is 0.1 g kg^{-1}. (c) As in (a) but for the potential energy flux and standard deviation of geopotential height σ_z $(=\sqrt{\overline{z'^2}})$ (solid line). Shown also is the vertically averaged geopotential height between the surface and 150 mb (dashed line). Contour interval for σ_z is 10 m and for geopotential height 100 m. (d) As in (a) but for the kinetic energy flux $(\overline{k'\mathbb{V}'})$. The solid lines are stream lines of the vertically averaged mean wind.

4.2. *Wintertime transient eddy fluxes of energy*

The vertically integrated transient eddy fluxes of all energy components ($c_p T$, Lq, gz, k) for winter (December–February) are given in Fig. 3. To consider the magnitudes first, $\bar{\mathbb{F}}_S^T$ is the largest (with a magnitude of 100–200 MW/m in northern Europe), $\bar{\mathbb{F}}_L^T$ and $\bar{\mathbb{F}}_P^T$ are somewhat smaller (about 50 MW/m) and $\bar{\mathbb{F}}_K^T$ is the smallest (about 25 MW/m). The flux $\bar{\mathbb{F}}_A^T$ is thus made up mainly of $\bar{\mathbb{F}}_S^T$.

$\bar{\mathbb{F}}_S^T$ and $\bar{\mathbb{F}}_L^T$ (Fig. 3a, b) show rather similar vector orientation which is characterized by a northward down-gradient flux and a component from the ocean to the land. These fluxes can qualitatively be understood as resulting from the large-scale mixing process, acting so as to smooth out the mean temperature and moisture gradient. As a detail, the effect of the Mediterranean on the moisture flux is seen at stations lying on its northern coast: $\bar{\mathbb{F}}_L^T$ vectors clearly indicate moisture transport by transient eddies out of the sea area.

The behaviour of the transient eddy flux of potential energy (Fig. 3c) shows a quasi-parallelism of $\bar{\mathbb{F}}_P^T$ with the isolines of geopotential variance. This is due to the predominance of the geostrophic part of the flux, which can be written

$$\overline{z'\mathbb{v}'_g} = \overline{z'\left(k \times \frac{g}{f}\nabla z\right)'} = \frac{g}{2f} k \times \nabla\overline{z'^2} \tag{5}$$

(Lau and Wallace, 1979). Although the fluxes are rather small compared with those of sensible heat and are generally zonal in character, the zonally averaged values of $\overline{z'v'}$ (which are entirely due to ageostrophic motion) play an important role in the maintenance of low-latitude large-scale eddies (Holopainen, 1969; Mak, 1969).

The $\bar{\mathbb{F}}_K^T$ vectors (Fig. 3d) approximately parallel the mean wind vectors. This may be understood by considering the climatology of the jet streams with their large value of specific kinetic energy. If the jet streams tend to have certain preferential directions (predominantly south-eastward over Europe) the $\overline{k'\mathbb{v}'}$ vectors will obviously have their main component in the same direction.

4.3. *Summertime transient eddy fluxes of energy*

The flux vectors $\bar{\mathbb{F}}_S^T$ and $\bar{\mathbb{F}}_L^T$ during summer (June–August) show (Fig. 4a, b) the same general down-gradient flux pattern as in winter. The main difference between winter and summer conditions is in the direction of the vectors: in summer the fluxes have a small component from the continent to the ocean. In northern Europe the flux vectors of sensible heat are about one-half the magnitude compared with those in winter. These differences are basically in accordance with a change in the baroclinity of the atmosphere over Europe from winter to summer: the reversal of the land–ocean temperature contrasts brings about a reversal of the longitudinal gradient of the mean temperature.

In the case of latent heat the vertical integrals strongly reflect the conditions prevailing below 850 mb and the effect of the underlying surface is pronounced. This can be seen in the behaviour of the direction of $\bar{\mathbb{F}}_L^T$ vectors, which during winter (Fig. 3b) show a tendency to west–east orientation reflecting the land–ocean contrast, especially in central Europe. In summer, however, the vector orientation is nearly meridional. This suggests that the temperature dependence of the moisture content of the air (and not so much the character of the underlying surface) dominates $\bar{\mathbb{F}}_L^T$.

Because the gradients of geopotential height variance field in summer are smaller than in winter, it is natural, in the light of eq. (5), that the transient eddy flux of potential energy (Fig. 4c) also has a smaller magnitude in summer than in winter. Also corresponding vectors of kinetic energy flux $\bar{\mathbb{F}}_K^T$ (Fig. 4d) are smaller in summer than in winter. As in winter, $\bar{\mathbb{F}}_K^T$ has also in summer nearly the same direction as the vertically averaged flow.

5. The anomalous flux of sensible heat by transient eddies near the tropopause over western Europe in winter

The meridional component of the transient eddy flux of sensible heat has received much attention in the literature because it is the quantity of primary importance when zonally averaged energy balance in the middle latitudes is involved. Geographically, this flux component is characterized by positive (northward flux) values practically everywhere in the atmosphere except in the upper troposphere, where it is negative (southward flux), in certain longitudinal sectors especially in winter.

The reversal of the sign of $\overline{T'v'}$ at about 500 mb and the tropopause level at some geographical locations was first discovered by Priestley (1949), who used radiosonde observations from one station in southern England in his study. Later investigations by Peixoto (1960), Newell et al. (1974), Lau (1978) and Lau and Wallace (1979) based on larger data sets have confirmed his findings. Lau (1978), who has used the largest data set so far, computed the eddy statistics separately for seven longitudinal sectors in the northern hemisphere based on NMC analyses for 11 winters. He found southward heat fluxes between 500 and 250 mb in the sectors of western continents and, to a minor extent, in eastern Asia.

The flux vectors $\overline{T'\mathbb{v}'}$ as computed from our data are shown in Fig. 5a for 300 mb and in Fig. 5b for 200 mb. It is seen that a southward or

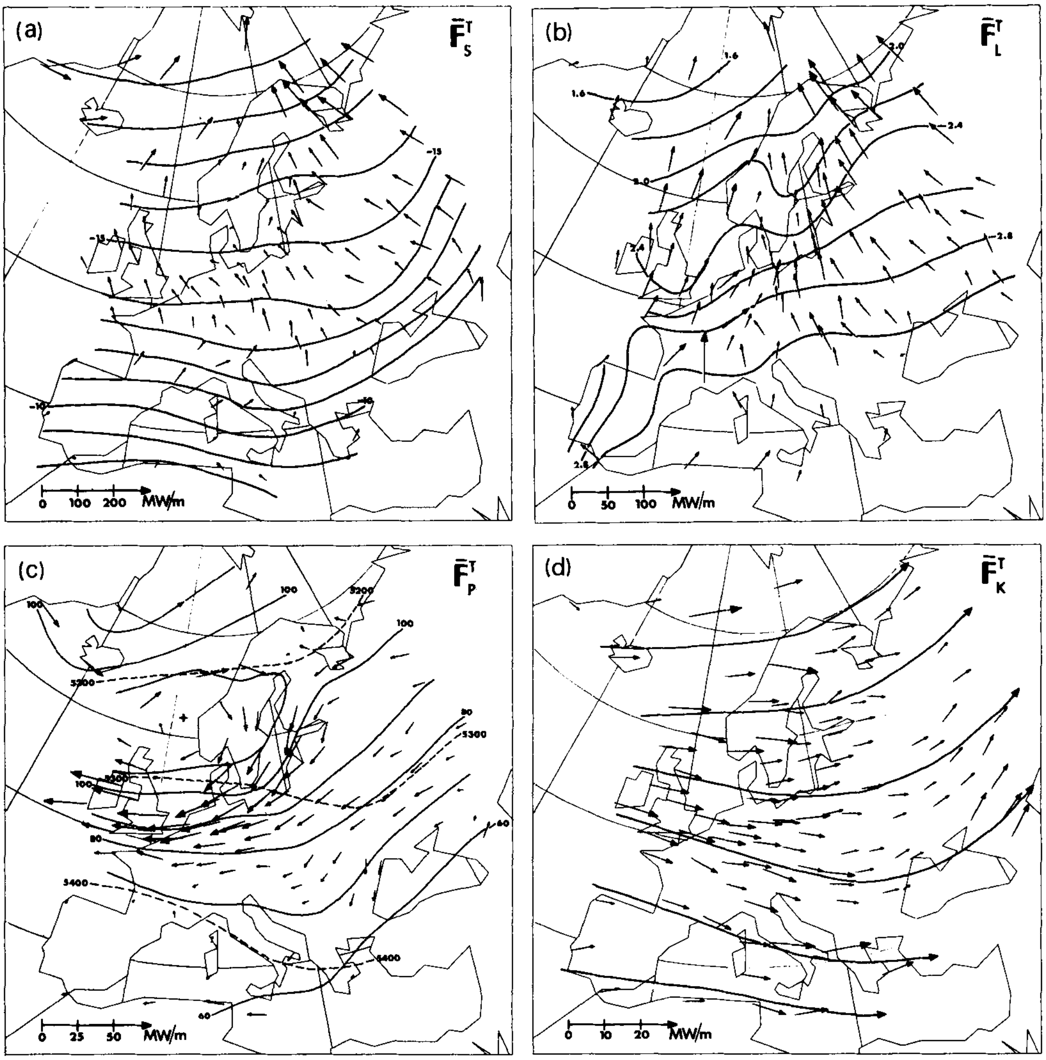

Fig. 4. Transient eddy energy fluxes in summer. (a) The vertically integrated transient eddy flux of sensible heat in summer and the analysis of the vertically averaged temperature between the surface and 150 mb for the period 1974–1976. Contour interval is 1 °C. (b) As in (a) but for the latent heat flux and specific humidity. Contour interval is 0.2 g kg^{-1}. (c) As in (a) but for the potential energy flux and standard deviation of geopotential height σ_z $(=\sqrt{\overline{z'^2}})$ (solid line). The vertically averaged geopotential height between the surface and 150 mb is also shown (dashed line). Contour interval for σ_z is 10 m and for geopotential height 100 m. (d) As in (a) but for the kinetic energy flux ($\overline{k'\mathbf{v}'}$). The solid lines are the stream lines of vertically averaged mean wind.

south-eastward flux is present at 300 mb over most of central Europe, whereas at 200 mb the flux is predominantly northward as it is in the lower troposphere (not shown). These findings agree with those reported by Lau and Wallace (1979) on the basis of nearly hemispheric (NMC) data; over Europe, however, our results have much higher resolution than those by Lau and Wallace.

According to Fig. 5a the main component of $\overline{T'\mathbf{v}'}$ at 300 mb is parallel to the mean isotherms, a

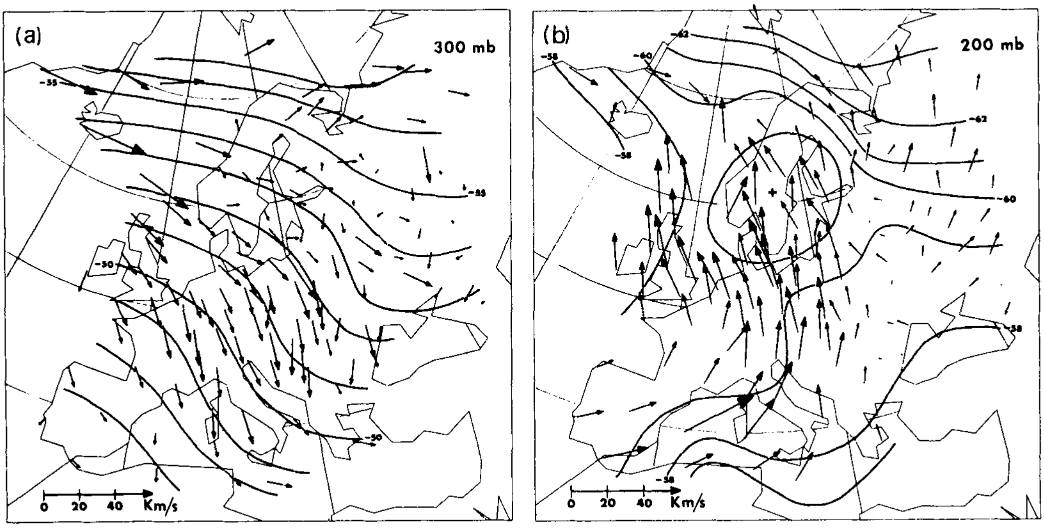

Fig. 5. The transient eddy flux of temperature ($\overline{T'\mathrm{v}'}$) and the field of mean temperature in winter: (a) at 300 mb and (b) at 200 mb.

situation different from that prevailing in the lower troposphere and in the vertical average (Fig. 3a). This flux can be visualized as arising as a result of fluctuations in a jet stream, with typical associated frontal structure, in the direction perpendicular to its axis. On the warmer side of the front in the middle and upper troposphere, velocity is typically higher than on the colder side at the same pressure level. This brings about a positive covariance between the local fluctuations of temperature and the wind component parallel to the front. The southward component of $\overline{T'\mathrm{v}'}$ seen in Fig. 5a is thus partly understandable in terms of the typical NW–SE orientation (over western Europe) of the upper-level front, which is naturally also responsible for the pattern of mean isotherms seen in Fig. 5a.

The above synoptic interpretation of one of the basic features of $\overline{T'\mathrm{v}'}$ seen in Fig. 5a is complementary to that of Lau and Wallace (1979), who argued that in the upper troposphere the behaviour of the transient disturbances is nearly equivalent-barotropic. This implies that $T' \simeq cz'$ (c = a positive constant) and, further, that $\overline{T'\mathrm{v}'} \simeq (cg/2f)\hat{k} \times \nabla\overline{z'^2}$ (see eq. (5)). Because $\overline{z'^2}$ has a maximum over the Atlantic west of Europe it is natural to have a considerable (non-divergent) component of $\overline{T'\mathrm{v}'}$ southward over western Europe.

An interesting feature in Fig. 5a is that $\overline{T'\mathrm{v}'}$ at 300 mb has not only a component parallel to the mean isotherms but clearly also an up-gradient component, i.e. a component towards higher mean temperature. The physical processes leading to this up-gradient flux at certain locations are not yet thoroughly solved. The problem can be approached by first investigating what frequencies contribute to this flux. The partitioning of $\overline{T'\mathrm{v}'}$ at 300 mb for winter conditions into contributions from periods shorter than 30 days ("synoptic eddies") and longer than 30 days is shown in Fig. 6. According to this figure it is mainly the synoptic eddy part of the flux that is directed up-gradient; the low-frequency part, which is likely to vary considerably from one 3-year period to another, has a much smaller magnitude and, over eastern Europe, even a component to the north.

Synoptic conditions, which at 300 mb seem to favour large negative deviations (from time mean values) of v and corresponding positive deviations of T, are the periods when horizontal shear lines with near-meridional orientation (with a large-amplitude pressure ridge westward from the shear line) are found on synoptic charts for the upper troposphere. In these situations strong northerly winds are often accompanied by temperatures which are high in comparison with those found eastward of the shear line. A warm upper

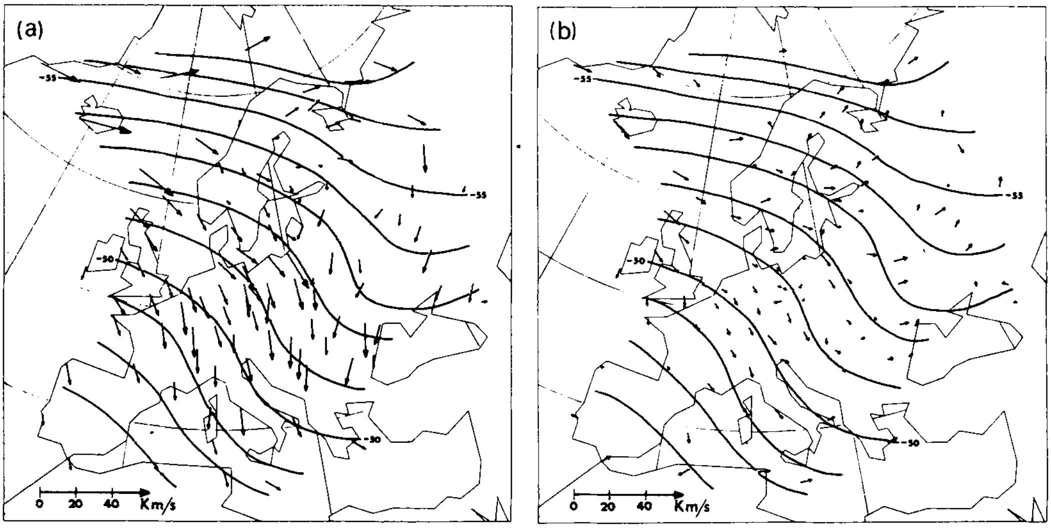

Fig. 6. Mean temperature (solid lines) at 300 mb in winter and contributions to the total transient eddy flux of temperature (see Fig. 5a) from (a) periods shorter than 30 days, (b) periods longer than 30 days.

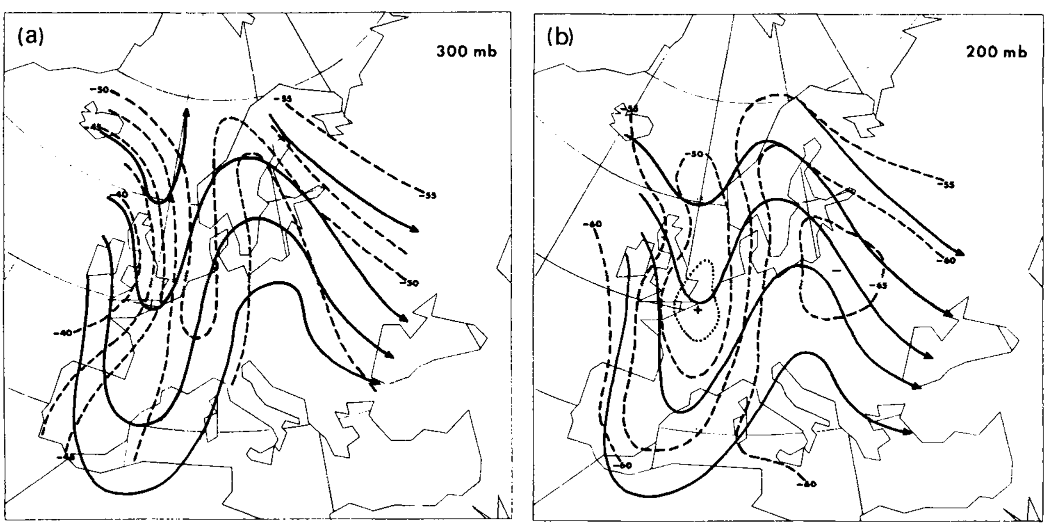

Fig. 7. The distribution of stream lines (solid lines) and temperature (dashed lines) on November 2, 1975, 00 GMT, (a) at 300 mb and (b) at 200 mb.

troposphere is typically connected with a colder stratosphere and vice versa (e.g. Palmén and Newton, 1969, ch. 7). Thus, at 200 mb where the wind structure is essentially the same as at 300 mb, a positive spatial covariance between T and v is expected around the shear line.

An example of this kind of situation is given in Fig. 7 which shows isotherms and stream lines at 300 and 200 mb on November 2, 1975 at 00 GMT over Europe. At 300 mb (Fig. 7a) a strong northerly flow is found above the British Isles, where the temperatures are relatively high compared to average conditions in the map area. Because the temperature wave is in front of the stream line wave, relatively cold temperatures are connected with southerly flow to the east of the shear line. Assuming a rough correspondence between time–mean and area–mean and the same for deviations (a kind of Taylor hypothesis), we can expect from this kind of situation a negative (and up-gradient) contribution to the transient eddy flux $\overline{T' v'}$. At 200 mb (Fig. 7b) the coldest temperatures are found in connection with northerly winds and thus a positive spatial covariance between T and v (and positive contribution to $\overline{T' v'}$) arises.

The recent studies by Blackmon et al. (1977) and Lau (1979) on the structure of transient disturbances show that these eddies are on the average characterized by smaller baroclinity in western continents and adjacent ocean areas than those in the western parts of the oceans. The westward tilt of moving disturbances in their active phase (over the western oceans) is considerably reduced as the disturbances move eastward and approach their dissipation phase, and may even reach a stage with eastward tilt (geopotential wave lagging behind the temperature wave).

Thus, the longitudinal variation of $\overline{T' v'}$ seems to depend upon the longitudinal variation of the typical phase of life cycle of large-scale disturbances, as experienced locally. The longitudinal sectors characterized by upper tropospheric southward transient eddy flux of sensible heat are those in which typically mature or decaying large-amplitude upper-levels waves occur, often connected with "blocking highs", "cut-off" lows and shear lines. Berggren et al. (1949) introduced a schematic model of the "crowding" of decaying waves over western Europe.

The observed up-gradient transient eddy flux of sensible heat in the upper troposphere is thus understandable in terms of a decaying baroclinic wave with a temperature wave ahead of the stream line wave, and is thus only one aspect of the decay process. However, as the example in Fig. 7 and that provided by Berggren et al. (1949) show, the actual flow patterns involved are not simple sine waves but complex non-linear features of the atmospheric large-scale turbulence.

6. Summary

Atmospheric fluxes of total energy and its components over Europe have been computed for the period 1974–1976. The main results may be summarized as follows:

(1) The flux associated with the time–mean motion makes the main contribution to the time–mean fluxes.
(2) The transient eddy fluxes of sensible and latent heat reflect the effect of large-scale atmospheric mixing acting to smooth out the contrasts of mean temperature and humidity. These fluxes are thus largely controlled by the local time–mean baroclinity of the atmosphere.
(3) Up-gradient transient eddy flux of sensible heat is observed in the upper troposphere above western Europe. This flux is found to be mainly due to atmospheric fluctuations with periods of less than 30 days. An example of synoptic conditions which statistically lead to a negative correlation between T and v is presented. This situation, quite common in western Europe, is characterized by the existence of large-amplitude waves and shear lines in the upper troposphere.
(4) The transient eddy flux of potential energy can be largely explained in terms of geopotential variance distribution. This implies that the flux is essentially determined by geostrophic winds. The pattern of the transient eddy flux of kinetic energy is very similar to that of the mean wind and shows that the jet streams with their large kinetic energies control this flux. Both of these fluxes are relatively unimportant from the point of view of total energy.

Divergences of the computed energy fluxes, important for understanding the role of large-scale atmospheric motion in the maintenance of the regional energy balance, will be discussed in a separate paper.

7. Acknowledgements

The authors are indebted to Professor E. Palmén for many illustrative discussions and for his interest in the present work. The valuable advice received at various stages of the data processing from the EOF group of the Department of Meteorology, University of Helsinki, is also gratefully acknowledged. Drafting of the final figures was done by Mr Pertti Nurmi and typing by Mrs Pirkko Saarikivi.

REFERENCES

Alestalo, M. 1979. Atmospheric energy fluxes over Europe. Licenciate thesis from Department of Meteorology, University of Helsinki.

Behr, H. D. and Speth, P. 1977. An investigation of the atmospheric heat and moisture balance in the Baltic Sea region. Part II: Heat balance. *Meteorol. Rdsch. 30*, 97–111.

Berggren, R., Bolin, B. and Rossby, C.-G. 1949. An aerological study of zonal motion, its perturbation and breakdown. *Tellus 1*, 14–37.

Blackmon, M. L. 1976. A climatological spectral study of the 500 mb geopotential height of the Northern Hemisphere. *J. Atmos. Sci. 33*, 1607–1623.

Blackmon, M. L., Wallace, J. M., Lau, N.-C. and Mullen, S. L. 1977. An observational study of the Northern Hemisphere wintertime circulation. *J. Atmos. Sci. 34*, 1040–1053.

Holopainen, E. O. 1969. On the maintenance of the atmosphere's kinetic energy over the Northern Hemisphere in winter. *PAGEOPH 77*, 104–121.

Holopainen, E. O. and Eerola, K. 1979. A diagnostic study of the long-term balance of kinetic energy of atmospheric large scale motion over the British Isles. *Q. J. Roy. Met. Soc. 105*, 849–858.

Kung, E. C. 1966. Large scale balance of kinetic energy in the atmosphere. *Mon. Wea. Rev. 94*, 627–640.

Lau, N.-C. 1978. On the three dimensional structure of the observed transient eddy statistics of the Northern Hemisphere wintertime circulation. *J. Atmos. Sci. 35*, 1900–1923.

Lau, N.-C. 1979. The structure and energetics of transient disturbances in the Northern Hemisphere wintertime circulation. *J. Atmos. Sci. 36*, 982–995.

Lau, N.-C. and Wallace, J. M. 1979. On the distribution of horizontal transports by transient eddies in the Northern Hemisphere wintertime circulation. *J. Atmos. Sci. 36*, 1844–1861.

Mak, M.-K. 1969. Laterally driven stochastic motions in the tropics. *J. Atmos. Sci. 26*, 41–64.

Newell, R. E., Kidson, J. W., Vincent, D. G. and Boer, G. J. 1972. *The general circulation of the tropical atmosphere and interactions with extratropical latitudes*. Vol. 1. Cambridge, Mass.: The MIT Press, 258 pp.

Newell, R. E. 1974. *The general circulation of the tropical atmosphere and interactions with extratropical latitudes*. Vol. 2. Cambridge, Mass.: The MIT Press, 371 pp.

Oort, A. H. and Rasmusson, E. M. 1971. *Atmospheric circulation statitstics*. NOAA Prof. Paper No. 5. Washington, D.C.: U.S. Government Printing Office, 323 pp.

Opsteegh, J. D. and van den Dool, H. M. 1979. A diagnostic study of the time–mean atmosphere over northwestern Europe during winter. *J. Atmos. Sci. 36*, 1862–1879.

Palmén, E. and Newton, C. W. 1969. *Atmospheric circulation systems: Their structure and physical interpretation.* International Geophysics Series 13. New York: Academic Press, 603 pp.

Peixoto, J. P. 1960. *Hemispheric temperature conditions during the year 1950.* Scientific report No. 4, Planetary circulations project, MIT, Dep. of Meteor., 211 pp.

Priestley, C. H. B. 1949. Heat transport and zonal stress between latitudes. *Q. J. Roy. Met. Soc. 75*, 28–40.

Spackmann, E. A. 1978. The compatibility of upper-air data. Part II: The compatibility and performance of radiosonde measurements of geopotential height in the lower stratosphere for 1975–76. *Tech. Note No. 163*, WMO—No. 512, 29–103.

Speth, P. 1978. Time-spectral analysis of large-scale eddy transport of sensible heat and momentum. *Contr. Atmos. Phys. 51*, 153–165.

ПОТОКИ ЭНЕРГИИ В АТМОСФЕРЕ НАД ЕВРОПОЙ

Горизонтальные потоки атмосферной энергии (явное и скрытое тепло, потенциальная и кинетическая энергия) вычисляются на европейских аэрологических станциях в слое от поверхности земли до уровня 150 мбар за период 1974–1976 г.г. Отдельно вычисляются вклады от среднего течения и от нестационарных вихрей. Главный акцент делается на вычисление потоков за счет нестационарных вихрей и на их физическую и синоптическую интерпретацию. Существенно, что проинтегрированные по вертикали потоки явного и скрытого тепла за счет нестационарных вихрей направлены по градиенту и отражает "перемешивание", вызываемое крупномасштабной атмосферной турбулентностью.

Найдено, что поток явного тепла за счет нестационарных вихрей в верхней тропосфере над западной Европой зимой направлен к югу и против градиента. Путем использования простой техники осреднения показано, что этот противоградиентный поток в основном обусловлен флуктуациями с периодом меньше месяца. Представлен синоптический пример, когда имеется волна с большой амплитудой, типичная для ситуации, в которой формируются отсеченные циклоны. В этом случае имеется отрицательная пространственная корреляция между температурой и меридиональной компонентой ветра. Явление такого типа, которое часто наблюдается в Западной Европе, частично ответственно за наблюдаемую противоградиентную компоненту потока явного тепла, создаваемого нестационарными вихрями.